

Localized wave solutions and interactions of the (2+1)-dimensional Hirota—Satsuma—Ito equation

Qiankun Gong(巩乾坤), Hui Wang(王惠), and Yunhu Wang(王云虎)

Citation: Chin. Phys. B, 2024, 33 (**4**): 040505. DOI: 10.1088/1674-1056/ad1f4c
Journal homepage: http://cpb.iphy.ac.cn; http://iopscience.iop.org/cpb

What follows is a list of articles you may be interested in

Different wave patterns for two-coupled Maccari's system with complex structure via truncated Painlevé approach

Hongcai Ma(马红彩), Xinru Qi(戚心茹), and Aiping Deng(邓爱平)
Chin. Phys. B, 2023, 32 (**12**): 120503. DOI: 10.1088/1674-1056/acf497

General *M*-lumps, *T*-breathers, and hybrid solutions to (2+1)-dimensional generalized KDKK equation

Peisen Yuan(袁培森), Jiaxin Qi(齐家馨), Ziliang Li(李子良), and Hongli An(安红利)
Chin. Phys. B, 2021, 30 (**4**): 040503. DOI: 10.1088/1674-1056/abcf9f

Deformed two-dimensional rogue waves in the (2+1)-dimensional Korteweg-de Vries equation

Yulei Cao(曹玉雷), Peng-Yan Hu(胡鹏彦), Yi Cheng(程艺), and Jingsong He(贺劲松)
Chin. Phys. B, 2021, 30 (**3**): 030503. DOI: 10.1088/1674-1056/abd15e

Localized characteristics of lump and interaction solutions to two extended Jimbo-Miwa equations

Yu-Hang Yin(尹宇航), Si-Jia Chen(陈思佳), and Xing Lü(吕兴)
Chin. Phys. B, 2020, 29 (**12**): 120502. DOI: 10.1088/1674-1056/aba9c4

Lump, lumpoff and predictable rogue wave solutions to a dimensionally reduced Hirota bilinear equation

Haifeng Wang(王海峰), Yufeng Zhang(张玉峰)
Chin. Phys. B, 2020, 29 (**4**): 040501. DOI: 10.1088/1674-1056/ab75d7

Localized wave solutions and interactions of the (2+1)-dimensional Hirota–Satsuma–Ito equation

Qiankun Gong(巩乾坤), Hui Wang(王惠)†, and Yunhu Wang(王云虎)

School of Science, Shanghai Maritime University, Shanghai 201306, *China*

(Received 2 December 2023; revised manuscript received 14 January 2024; accepted manuscript online 17 January 2024)

This paper studies the (2+1)-dimensional Hirota–Satsuma–Ito equation. Based on an associated Hirota bilinear form, lump-type solution, two types of interaction solutions, and breather wave solution of the (2+1)-dimensional Hirota–Satsuma–Ito equation are obtained, which are all related to the seed solution of the equation. It is interesting that the rogue wave is aroused by the interaction between one-lump soliton and a pair of resonance stripe solitons, and the fusion and fission phenomena are also found in the interaction between lump solitons and one-stripe soliton. Furthermore, the breather wave solution is also obtained by reducing the two-soliton solutions. The trajectory and period of the one-order breather wave are analyzed. The corresponding dynamical characteristics are demonstrated by the graphs.

Keywords: lump solution, rogue wave solution, breather wave solution, (2+1)-dimensional Hirota–Satsuma–Ito equation

PACS: 05.45.Yv, 02.30.Ik, 02.30.Jr **DOI:** 10.1088/1674-1056/ad1f4c

1. Introduction

In recent decades, nonlinear partial differential equations (NPDEs) have found extensive applications in oceanography, quantum mechanics, biology, and geology. Notably, ocean represents a complex system, including ocean fluid dynamics, wave dynamics, marine ecosystems, and so on. NPDEs play a pivotal role in the field of marine science, with significant implications for navigation, coastal engineering, ocean resource management, and fisheries, among others. For instance, the Navier–Stokes equations[1–3] and the Korteweg–de Vries equation[4–6] are employed via numerical simulations to address practical issues by studying nonlinear internal waves.

In the field of nonlinear wave, finding various of localized wave solutions of the NPDEs has been a focal point of research for many scholars. Examples of such solutions include soliton solutions,[7–15] breather wave solutions,[16–20] lump solutions,[21–25] rogue wave solutions,[26,27] and soliton–cnoidal wave interaction solutions.[28,29] In the ocean, lump solutions are commonly used to describe phenomena such as breaking waves in the ocean and sharp peaks in tides.[30] Breather wave solutions can be utilized to simulate and study the long-lasting characteristics of waves, such as tidal waves and internal waves.[31] Currently, numerous methods for solving NPDEs have been developed, such as the Hirota bilinear method,[32] the Darboux transformation method,[33] the inverse scattering transformation method,[34] the Bäcklund transformation method.[35]

In 1981, Hirota and Satsuma introduced the Hirota–Satsuma (HS) equation to model shallow water waves through the Bäcklund transformation of the Boussinesq equation.[36] The HS equation provides a description of the propagation of unidirectional shallow water waves and the interaction between two long waves with different dispersion relations. The HS equation reads

$$u_t = u_{xxt} + 3uu_t - 3u_x v_t - u_x, \quad v_x = -u, \tag{1}$$

which can also be written as the following Hirota bilinear form:

$$\left(D_t D_x^3 - D_t D_x - D_x^2\right) f \cdot f = 0, \tag{2}$$

by using a transformation $u = 2(\ln f)_{xx}$. As an integrable (2+1)-dimensional extension of Eq. (1), the (2+1)-dimensional Hirota–Satsuma–Ito (HSI) equation reads[37–39]

$$w_t = u_{xxt} + 3uu_t - 3u_x v_t + \alpha u_x, \quad w_x = -u_y, \quad v_x = -u, \tag{3}$$

with the following bilinear form

$$(D_t D_x^3 + D_t D_y + \alpha D_x^2) f \cdot f = 0, \tag{4}$$

where α is a real nonzero constant and the Hirota bilinear operators D are defined as follows:

$$\begin{aligned} &(D_x^k D_y^m D_t^n f \cdot g)(x,y,t) \\ =\ &(\partial_x - \partial_{x'})^k \left(\partial_y - \partial_{y'}\right)^m (\partial_t - \partial_{t'})^n \\ &\times f(x,y,t) g\left(x',y',t'\right)\big|_{x'=x,y'=y,t'=t}. \end{aligned} \tag{5}$$

Soliton solutions exhibit exponential localization along specific directions and can be generated through the utilization of Hirota bilinear forms. Compared to soliton solutions, lump solutions exhibit localized and algebraically decaying properties in all spatial directions. Constructing the lump solutions of NPDEs by using Hirota bilinear forms or even generalized bilinear forms[40] is a hot topic. In recent years, significant progress has been made in constructing lump solutions for NPDEs based on the Hirota bilinear method. This

†Corresponding author. E-mail: hwang@shmtu.edu.cn

© 2024 Chinese Physical Society and IOP Publishing Ltd

method was introduced by Ma in 2015,[21] and then further developed to find various of interactions solutions.[41] Breather wave is a kind of important nonlinear localized waves that exhibit periodic behavior which can be derived by using the complexification method.[16–19] In this paper, the seed solution of HSI Eq. (3) is introduced into the bilinear form of the HSI Eq. (3), and then lump-type solution, interaction solutions, and breather wave solution of the HSI Eq. (3) are studied.

The organization of this paper is as follows. Section 2 gives the lump-type solution via a quadratic function. Section 3 gives the interaction solutions between lump solitons and one-stripe soliton via combining quadratic functions with exponential functions, whose interaction process produced the fusion and fission. Section 4 gives the interaction solutions between one-lump soliton and a pair of resonance stripe solitons via a combination of positive quadratic function and a hyperbolic cosine function. Section 5 gives the breather wave solution via the complexification method. Section 6 makes the conclusion.

2. Lump solution

In order to obtain lump solution to the HSI Eq. (3), we first apply the following transformation:

$$u = u_0 + 2(\ln f)_{xx}, \tag{6}$$

to transform HSI equation (3) into the bilinear form

$$(D_x^3 D_t + 3u_0 D_x D_t + \alpha D_x^2 + D_y D_t) f \cdot f = 0, \tag{7}$$

where f is a real function, and u_0 serves as a seed solution for arbitrary constants.

By taking function f as follows:

$$f = g^2 + h^2 + a_9, \tag{8}$$

with

$$g = a_1 x + a_2 y + a_3 t + a_4,$$
$$h = a_5 x + a_6 y + a_7 t + a_8,$$

where a_i $(1 \le i \le 9)$ are real parameters to be determined. By substituting Eq. (8) into Eq. (7), we have

$$a_2 = \frac{\alpha a_3(a_3a_5 - a_1^2) - (3a_3^2u_0 + 2a_5a_7\alpha + 3a_7^2u_0)a_1}{a_3^2 + a_7^2},$$
$$a_9 = -\frac{3(a_3^2 + a_7^2)(a_1^2 + a_5^2)(a_1a_3 + a_5a_7)}{(a_1a_7 - a_3a_5)^2\alpha},$$
$$a_6 = \frac{\alpha a_7(a_1^2 - a_5^2) - (2a_1a_3\alpha + 3a_3^2u_0 + 3a_7^2u_0)a_5}{a_3^2 + a_7^2},$$

which need to satisfy the following constraint conditions:

$$a_1a_7 - a_3a_5 \neq 0,\ \alpha(a_1a_3 + a_5a_7) < 0, \tag{9}$$

to ensure that the corresponding solution f is analytic and positive.

Under the transformation (6), we obtain the following lump-type solution:

$$u = u_0 + \frac{1}{f^2}\big[(g^2 - h^2)(4a_5^2 - 4a_1^2) + a_9(4a_1^2 + 4a_5^2) - 16a_1a_5gh\big]. \tag{10}$$

Clearly, it is found that solution (10) approaches 0 at infinity

$$\lim_{x^2+y^2\to\infty} u = 0, \quad \text{when } u_0 = 0. \tag{11}$$

This result shows that the solution (10) is spatially localized when $u_0 = 0$, and therefore it can be regarded as the lump-type solution.

By taking $a_1 = -3$, $\alpha = a_5 = a_7 = a_8 = 1$, $a_3 = a_4 = 2$, the lump-type solution (10) can be further concretized into the following form:

$$u = \frac{M_1 + M_2 + M_3}{M_4}, \tag{12}$$

where

$$\begin{aligned}
M_1 &= 324u_0^5y^4 + 216u_0^4y^3(t - 2x - 2y + 1) \\
&\quad + 72u_0^3y^2\big[4y^2 + (-2t + 6x - 2)y \\
&\quad + 3x(x - t - 1) + (t + 1)^2 + 3\big], \\
M_2 &= 12u_0^2y\big[-8y^3 + (4t - 16x + 4)y^2 \\
&\quad + \big(-12x^2 + (8t + 8)x - 2t^2 - 4t - 26\big)y \\
&\quad + (t - 2x + 1)\big(2x^2 + (-2t - 2)x + t^2 + 2t + 7\big)\big], \\
M_3 &= u_0\big[16y^4 + 32xy^3 + \big(32x^2 - 16x(t + 1) \\
&\quad + 8t^2 + 16t + 152\big)y^2 + \big(16x^3 - 16x^2(t + 1) \\
&\quad + (8t^2 + 16t + 152)x - 48t - 48\big)y \\
&\quad + \big(2x^2 - 2x(t + 1) + t^2 + 2t + 7\big)^2\big] \\
&\quad + 32y(t - x + 1) + 48 - 16x^2 + 16x(t + 1), \\
M_4 &= \big[18u_0^2y^2 + 6u_0y(t - 2x - 2y + 1) + 4y^2 \\
&\quad + 4xy + 2x^2 - 2x(t + 1) + t^2 + 2t + 7\big]^2.
\end{aligned}$$

By solving the system $u_x = 0$, $u_y = 0$, we obtained the position of the lump wave as follows:

$$x(t) = -\frac{3}{2}tu_0 - \frac{3}{2}u_0 + t + 1, \quad y(t) = -\frac{t}{2} - \frac{1}{2}. \tag{13}$$

Therefore, the trajectory of the lump wave can be described as

$$y = \frac{x}{3u_0 - 2}. \tag{14}$$

It is evident that there exist three extremum points of u

$$(x_{u_1}, y_{u_1}) = \Big(-\frac{3}{2}tu_0 - \frac{3}{2}u_0 + t + 1, -\frac{t}{2} - \frac{1}{2}\Big), \tag{15a}$$
$$(x_{u_2}, y_{u_2}) = \Big(-\frac{3}{2}tu_0 - \frac{3}{2}u_0 + t - 2, -\frac{t}{2} - \frac{1}{2}\Big), \tag{15b}$$
$$(x_{u_3}, y_{u_3}) = \Big(-\frac{3}{2}tu_0 - \frac{3}{2}u_0 + t + 4, -\frac{t}{2} - \frac{1}{2}\Big), \tag{15c}$$

and the lump-type solution (12) has two troughs at points $(-\frac{3}{2}tu_0-\frac{3}{2}u_0+t-2,-\frac{t}{2}-\frac{1}{2})$ and $(-\frac{3}{2}tu_0-\frac{3}{2}u_0+t+4,-\frac{t}{2}-\frac{1}{2})$, one peak at point $(-\frac{3}{2}tu_0-\frac{3}{2}u_0+t+1,-\frac{t}{2}-\frac{1}{2})$. The peak of u has a value of $u_{\max}$, and two troughs of u with a same value of $u_{\min}$ as follows:

$$u_{\max}=u_0+\frac{4}{3},\quad u_{\min}=u_0-\frac{1}{6}. \tag{16}$$

The three images labeled (a), (b), and (c) in Fig. 1 and Fig. 2 respectively depict the three-dimensional (3D) plots and the corresponding density plots for the lump-type solution (12) when $u_0=0.3$, $t=-30$, 0, 30. Figure 2(d) represents the trajectory of the lump wave as it moves along $y=-x/1.1$.

When $u_0=1$, the trajectory of the lump wave changes to $y=x$, while other characteristics are similar to those of Figs. 1 and 2, which are shown in Figs. 3 and 4. Through theoretical analysis and graphical display, it is concluded that the seed solution u_0 significantly influences both the extreme value and the trajectory of the lump wave.

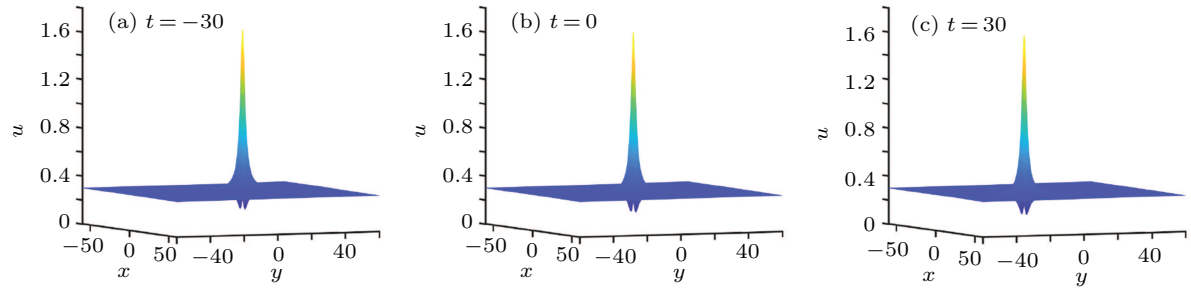


Fig. 1. The 3D plots of lump-type solution (12) with $u_0=0.3$, $a_1=-3$, $\alpha=a_5=a_7=a_8=1$, $a_3=a_4=2$.

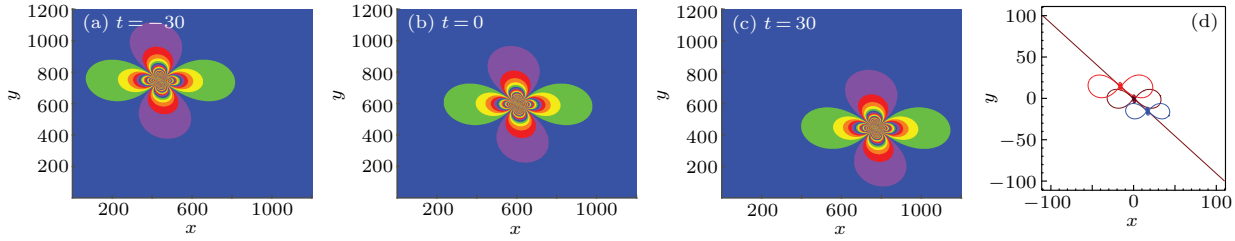


Fig. 2. Corresponding density plots and path plots for Fig. 1.

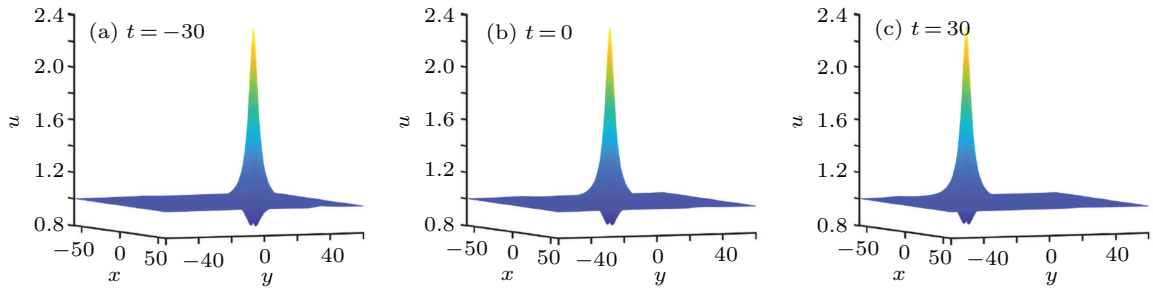


Fig. 3. The 3D plots of the lump-type solution (12) with $a_1=-3$, $u_0=\alpha=a_5=a_7=a_8=1$, $a_3=a_4=2$.

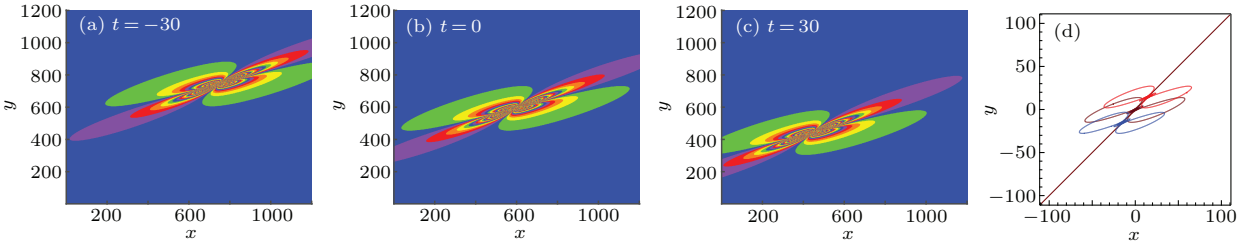


Fig. 4. Corresponding density plots and path plots for Fig. 3.

3. Fusion and fission phenomena

In order to obtain the interaction solution between lump solitons and one-stripe soliton for HSI Eq. (3), we consider the function f in Eq. (7) to be

$$f=g^2+h^2+k\exp(k_1x+k_2y+k_3t)+a_9, \tag{17}$$

with

$$g=a_1x+a_2y+a_3t+a_4,\quad h=a_5x+a_6y+a_7t+a_8,$$

where a_i $(1\le i\le 9)$ and k, k_j $(1\le j\le 3)$ are real param-

eters that will be determined later. By performing symbolic computation and directly substituting Eq. (17) into Eq. (7), the following results are obtained:

$$\begin{aligned}
&\alpha = -\frac{3k_3(a_1^2k_3^2+a_7^2k_1^2)}{4k_1a_7^2},\\
&a_2 = \frac{3a_1(a_1^2k_3^2-3a_7^2k_1^2-4a_7^2u_0)}{4a_7^2}, \quad a_3 = \frac{a_1k_3}{k_1},\\
&a_5 = -\frac{a_7k_1}{k_3}, \quad a_6 = -\frac{3k_1(3a_1^2k_3^2-a_7^2k_1^2-4a_7^2u_0)}{4k_3a_7},\\
&a_9 = \frac{a_1^4k_3^4-k_1^4a_7^4}{k_1^2k_3^4a_1^2}, \quad k_2 = \frac{k_1(3a_1^2k_3^2-a_7^2k_1^2-12a_7^2u_0)}{4a_7^2},
\end{aligned} \tag{18}$$

which must satisfy the following constraint conditions:

$$k_1k_3a_1a_7 \neq 0, \quad |a_1k_3| > |a_7k_1|, \tag{19}$$

to ensure that the corresponding solution f is analytic and positive.

Under the transformation (6), we have

$$\begin{aligned}
u = u_0 + \frac{1}{f^2}\{&2k\exp(k_1x+k_2y+k_3t)\big[2(a_1^2+a_5^2)\\
&+k_1^2(g^2+h^2+a_9)-4k_1(a_1g+a_5h)\big]\\
&+4a_1^2(h^2-g^2+a_9)+4a_5^2(g^2-h^2+a_9)\\
&-16a_1a_5gh\}.
\end{aligned} \tag{20}$$

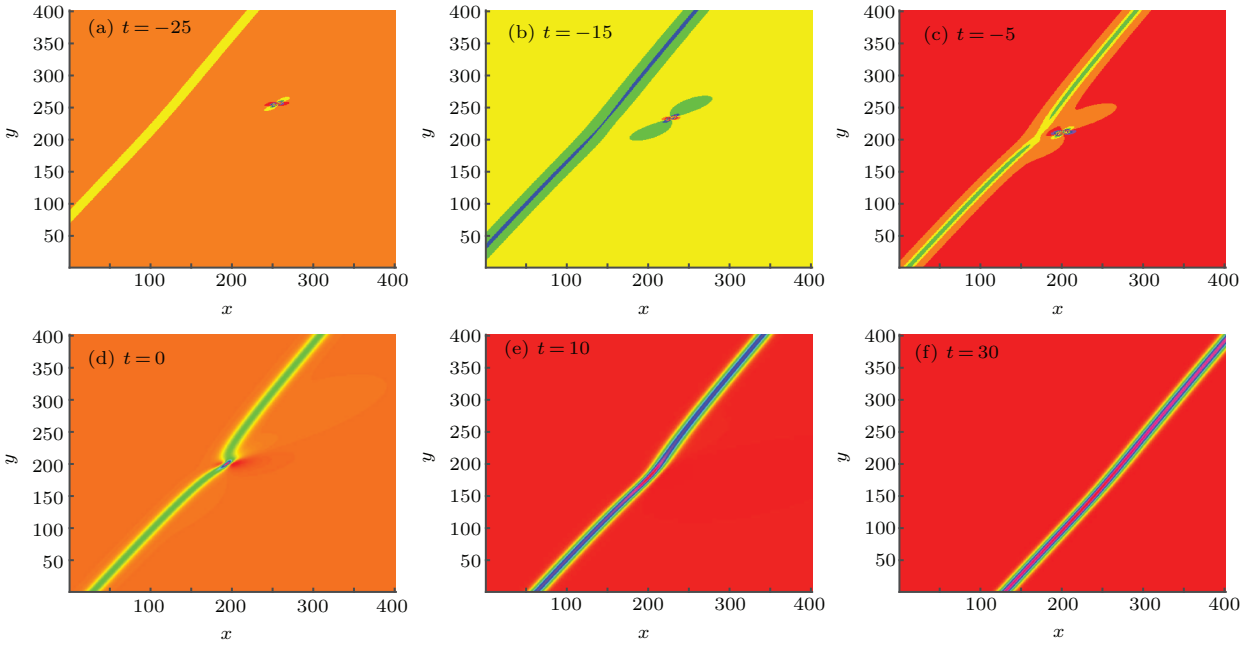


Fig. 5. Fusion phenomenon of the solution (20) with $u_0 = 0.4$, $a_1 = a_7 = k = k_3 = 1$, $a_5 = 2$, $a_4 = 3$, $a_8 = 4$, $k_1 = -1$.

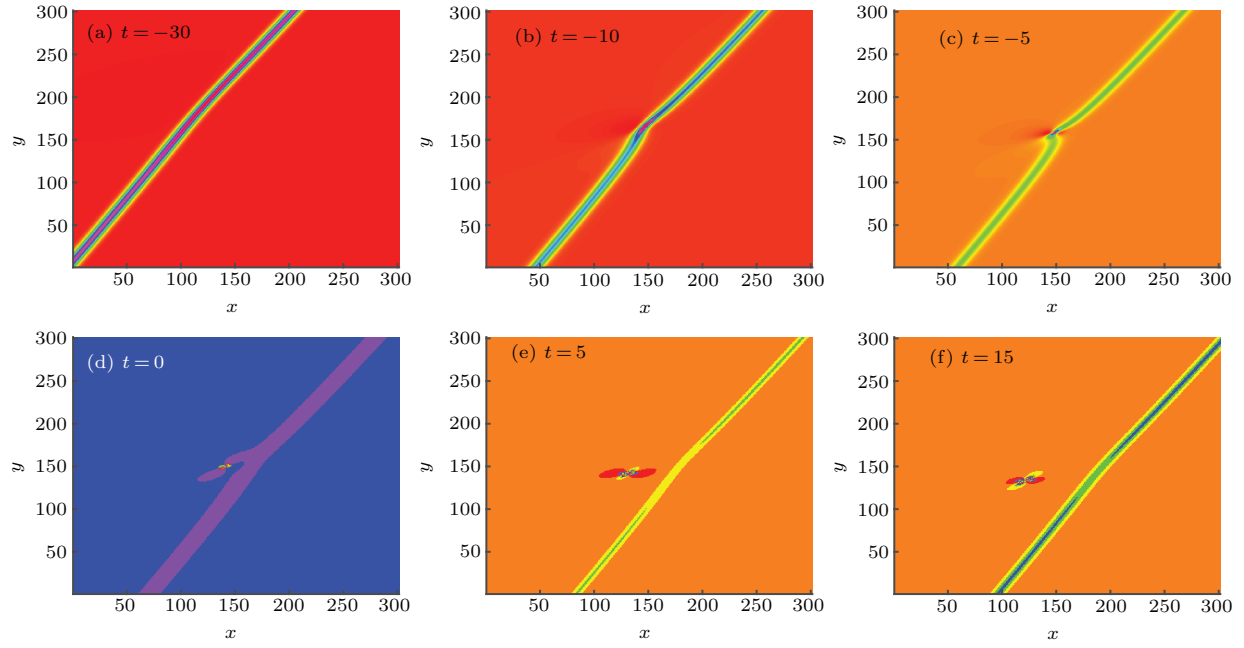


Fig. 6. Fission phenomenon of the solution (20) with $u_0 = 0.4$, $a_1 = a_7 = k = k_1 = 1$, $a_5 = 2$, $a_4 = 3$, $a_8 = 4$, $k_3 = -1$.

Figure 5 shows the dynamic performance of fusion phenomenon. The dynamic plots associated with solution (20) demonstrate that at $t=-25$, both lump solitons and one-stripe soliton exist simultaneously. As time evolving, the one-stripe soliton moves faster than lump solitons. At $t=30$, the one-stripe soliton dominates and engulfs the lump solitons. It is found that parameters k_1 and k_3 have an important effect on fusion and fission. In fact, fusion phenomenon occurs when $k_1=-1$, $k_3=1$. In contrast, fission occurs with $k_1=1$, $k_3=-1$.

It is evident from the Fig. 6 that at $t=-30$, one-stripe soliton exists. As time evolving, the one-stripe soliton undergoes decomposition, ultimately resulting in the formation of lump solitons and one-stripe soliton.

The aforementioned two phenomena exhibit similarity to soliton fusion and fission, which have already been theoretically discovered.[42,43] The results in this part show that dynamic characteristics of the solution (20) fully indicate that the interaction of lump solitons and one-stripe soliton can also produce fusion and fission phenomena.

4. Rogue wave solution

To search for rogue wave solution from Eq. (7), we take f as a combination of a positive quadratic function and a hyperbolic cosine function

$$f=g^2+h^2+k\cosh(k_1x+k_2y+k_3t)+a_9, \tag{21}$$

where

$$g=a_1x+a_2y+a_3t+a_4,\quad h=a_5x+a_6y+a_7t+a_8,$$

and a_i $(1\le i\le 9)$ and k, k_j $(1\le j\le 3)$ are parameters to be determined. By substituting Eq. (21) into Eq. (7) and performing a direct calculation, we obtain the following result:

$$\begin{aligned}
&a_2=-\frac{a_1(9k_3^2u_0+4\alpha^2)}{3k_3^2},\quad a_3=\frac{3a_1k_3^2}{4\alpha},\\
&a_6=-\frac{a_5(9k_3^2u_0+4\alpha^2)}{3k_3^2},\quad a_7=\frac{3a_5k_3^2}{4\alpha},\\
&k_1=-\frac{4\alpha}{3k_3},\quad k=\frac{9k_3^2(a_1^2+a_5^2)}{8\alpha^2},\\
&k_2=\frac{4\alpha(27k_3^2u_0+4\alpha^2)}{27k_3^2},
\end{aligned}\tag{22}$$

which needs to satisfy the constraint conditions

$$k_3a_1a_5\alpha\neq 0,\quad a_9>0. \tag{23}$$

Under the transformation (6), we obtain the following solution:

$$\begin{aligned}
u=\ & u_0+\frac{1}{f^2}\{2k\cosh(k_1x+k_2y+k_3t)\\
&\times\left[k_1^2(g^2+h^2+a_9)+2(a_1^2+a_5^2)\right]\\
&-8kk_1(ga_1+ha_5)\sinh(k_1x+k_2y+k_3t)-16a_1a_5gh\\
&+4a_1^2(h^2-g^2+a_9)+4a_5^2(g^2-h^2+a_9)\}.
\end{aligned}\tag{24}$$

The 3D plots in Fig. 7 displays the entire process of the creation and disappearance of the rogue wave. When $t=-60$, there are only two stripe solitons present. When $t=-20$, one of the stripe solitons generates a small wave packet. Immediately after, when $t=0$, the amplitude and energy of the lump soliton reach its maximum values, and it is positioned in the middle of the two resonance stripe solitons. As time progresses, the lump soliton moves towards the other stripe soliton and finally disappears, transforming into two resonance stripe solitons.

The observations from Fig. 7 indicates that, except for a specific time and fixed position, the presence of two resonance stripe solitons prevents the occurrence of the lump soliton. This suggests that the lump soliton can transform into a high-amplitude rogue wave at a suitable time and location.

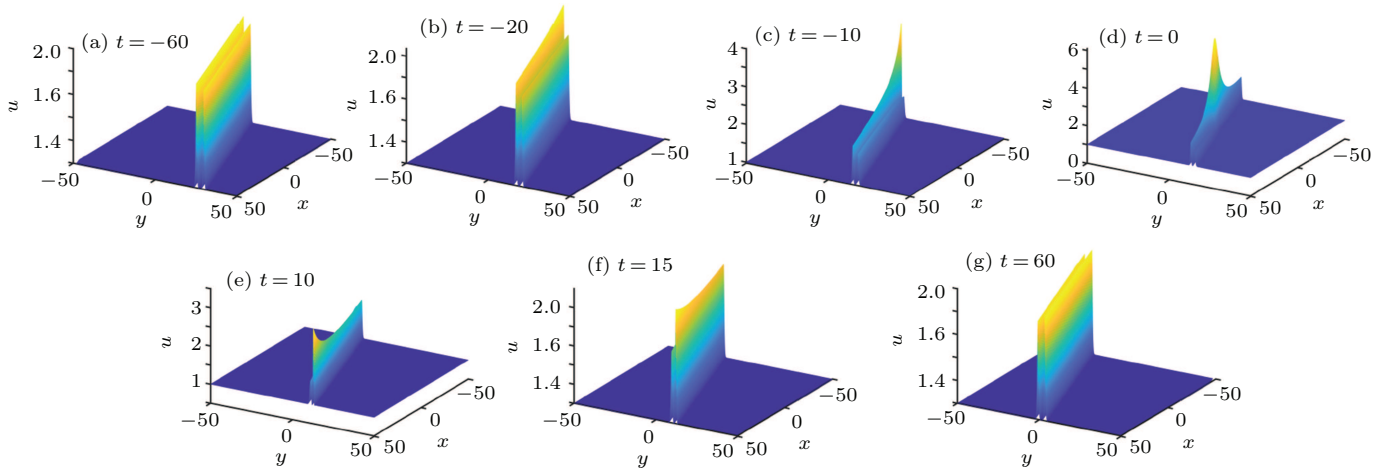


Fig. 7. Rogue wave phenomenon excited by solution (24) with $u_0=\alpha=k_3=a_8=1$, $a_1=a_9=2$, $a_4=a_5=3$.

5. Breather wave solution

It is well known that the two-soliton solution of HSI Eq. (3) can be directly obtained via bilinear equation (7)

$$\begin{aligned} &u = u_0 + 2(\ln f)_{xx}, \\ &f = 1 + \exp(\xi_1) + \exp(\xi_2) + A_{12}\exp(\xi_1+\xi_2), \end{aligned} \tag{25}$$

where

$$\begin{aligned} &A_{12} = \frac{k_1^4 - 3k_1^3k_2 + k_1^2m_1 - 3k_2k_1m_2 + k_2^4 + k_2^2m_3 + (p_1-p_2)^2}{k_1^4 + 3k_1^3k_2 + k_1^2m_1 + 3k_2k_1m_2 + k_2^4 + k_2^2m_3 + (p_1-p_2)^2}, \\ &\xi_i = k_i\left(x + p_i y - \frac{\alpha}{k_i^2 + 3u_0 + p_i}t\right) + \xi_i^0, \quad 1 \le i \le 2, \end{aligned} \tag{26}$$

and $m_1 = 4k_2^2 + 2p_1 + p_2 + 9u_0$, $m_2 = k_2^2 + p_1 + p_2 + 6u_0$, $m_3 = p_1 + 2p_2 + 9u_0$. Here k_i, p_i, ξ_i^0 $(1 \le i \le 2)$ are arbitrary real-valued constants. Based on the complexification method, suppose that

$$\begin{aligned} &k_1 = a_1 + \mathrm{i}b_1, \quad k_2 = a_1 - \mathrm{i}b_1, \\ &p_1 = c_1 + \mathrm{i}d_1, \quad p_2 = c_1 - \mathrm{i}d_1, \quad \xi_1^0 = 0, \quad \xi_2^0 = 0, \end{aligned} \tag{27}$$

then we have

$$\begin{aligned} &\xi_1 = \xi_2^* = R_1 + \mathrm{i}I_1, \\ &\alpha_{12} = \frac{a_1^2b_1^2 - 3b_1^4 + a_1b_1d_1 + 3b_1^2c_1 + 9b_1^2u_0 + d_1^2}{a_1^2b_1^2 - 3a_1^4 + a_1b_1d_1 - 3a_1^2c_1 - 9a_1^2u_0 + d_1^2}, \end{aligned} \tag{28}$$

where

$$\begin{aligned} R_1 = \mathrm{Re}(\xi_1) &= \frac{1}{Q_1}\big[a_1^5(c_1y+x) - a_1^4b_1d_1y + a_1^3Q_2 \\ &\quad + a_1^2Q_3 + a_1Q_4 - b_1d_1Q_5\big], \\ I_1 = \mathrm{Im}(\xi_1) &= \frac{1}{Q_1}\big[b_1^5(-c_1y-x) - b_1^4a_1d_1y + b_1^3P_1 \\ &\quad - b_1^2P_2 + b_1P_3 - a_1d_1P_4\big], \end{aligned} \tag{29}$$

with

$$\begin{aligned} Q_1 &= a_1^4 + a_1^2(2b_1^2 + 2c_1 + 6u_0) + 4a_1b_1d_1 \\ &\quad + b_1^4 - b_1^2(2c_1 + 6u_0) + 6c_1u_0 + d_1^2 + 9u_0^2, \\ Q_2 &= 2b_1^2(c_1y+x) + 2c_1y(c_1+3u_0) - \alpha t + 2c_1x + 6u_0x, \\ Q_3 &= b_1d_1(4x - 2b_1^2y + 2c_1y - 6u_0y), \\ Q_4 &= b_1^4(c_1y+x) \\ &\quad - b_1^2\big[2y(c_1^2 + 3c_1u_0 + 2d_1^2) + \alpha t + 2c_1x + 6u_0x\big] \\ &\quad + c_1y(c_1^2 + 6c_1u_0 + d_1^2 + 9u_0^2) + c_1^2x \\ &\quad + c_1(-\alpha t + 6u_0x) - 3tu_0\alpha + d_1^2x + 9u_0^2x, \\ Q_5 &= b_1^4y - 2b_1^2y(c_1 + 3u_0) \\ &\quad + y(c_1^2 + 6c_1u_0 + d_1^2 + 9u_0^2) + \alpha t, \\ P_1 &= -2a_1^2(c_1y+x) + 2c_1y(c_1+3u_0) - \alpha t + 2c_1x + 6u_0x, \\ P_2 &= a_1d_1(4x + 2a_1^2y + 2c_1y - 6u_0y), \\ P_3 &= a_1^4(-c_1y - x) \\ &\quad - a_1^2\big[2y(c_1^2 + 3c_1u_0 + 2d_1^2) + \alpha t + 2c_1x + 6u_0x\big] \\ &\quad - c_1y(c_1^2 + 6c_1u_0 + d_1^2 + 9u_0^2) - c_1^2x \\ &\quad + c_1(\alpha t - 6u_0x) + 3tu_0\alpha - d_1^2x - 9u_0^2x, \\ P_4 &= a_1^4y + 2a_1^2y(c_1 + 3u_0) \\ &\quad + y(c_1^2 + 6c_1u_0 + d_1^2 + 9u_0^2) + \alpha t. \end{aligned}$$

Under the conditions of Eqs. (27)–(29), the breather wave solution is $u_b = u_0 + 2(\ln f)_{xx}$, and we have

$$f = 1 + 2\exp(R_1)\cos(I_1) + \alpha_{12}\exp(2R_1), \tag{30}$$

from which the corresponding one-order breather wave solution of HSI Eq. (3) can be obtained.

The trajectory of the breather wave can be represented as a line L on the (x,y)-plane for a specific time t, and it is defined by

$$\begin{aligned} &a_1^5(c_1y+x) - a_1^4b_1d_1y + a_1^3Q_2 + a_1^2Q_3 \\ &+ a_1Q_4 - b_1d_1Q_5 = 0. \end{aligned} \tag{31}$$

The period of u is $T_y = -2\pi a_1/(a_1^2+b_1^2)d_1$ along the y direction and $T_x = 2\pi(a_1c_1 - b_1d_1)/(a_1^2+b_1^2)d_1$ for the x direction. Then, the distance between the two most neighboring peaks in u_b can be expressed as follows:

$$T = \sqrt{\frac{4\pi^2(a_1c_1 - b_1d_1)^2}{(a_1^2+b_1^2)^2d_1^2} + \frac{4\pi^2a_1^2}{(a_1^2+b_1^2)^2d_1^2}}. \tag{32}$$

T represents the period of an one-order breather wave along its trajectory. Furthermore, the forward speed of the one-order breather wave is determined to be

$$\begin{aligned} v_x &= \frac{\alpha\big[a_1^2d_1 + 2a_1b_1c_1 - d_1(b_1^2 - 2c_1 - 3u_0)\big]}{d_1x\big[a_1^4 + 2a_1^2(b_1^2 + c_1 + 3u_0) + 4a_1b_1d_1 - 2b_1^2(c_1+3u_0) + (c_1+3u_0)^2 + d_1^2\big]}, \\ v_y &= \frac{-2a_1b_1\alpha - d_1\alpha}{d_1y\big[a_1^4 + 2a_1^2(b_1^2 + c_1 + 3u_0) + 4a_1b_1d_1 - 2b_1^2(c_1+3u_0) + (c_1+3u_0)^2 + d_1^2\big]}. \end{aligned} \tag{33}$$

Here, v_x and v_y represent the velocities in the x direction and y direction, respectively.

Figures 8 and 9 demonstrate that the trajectory of the breather wave exhibits noticeable translational shifts, while the shape and speed remain unchanged during the shifting process. From the results shown in Eqs. (32), (33) and Figs. 8–11, we can obviously reach the conclusion that the seed solution u_0 only influences the speed of the breather wave but does not affect the period.

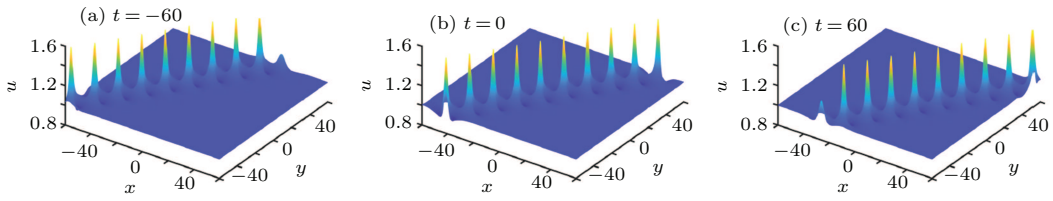


Fig. 8. Breather wave excited by the solution u_b with $u_0=\alpha=1$, $a_1=b_1=0.2$, $c_1=0.5$, $d_1=1.2$.

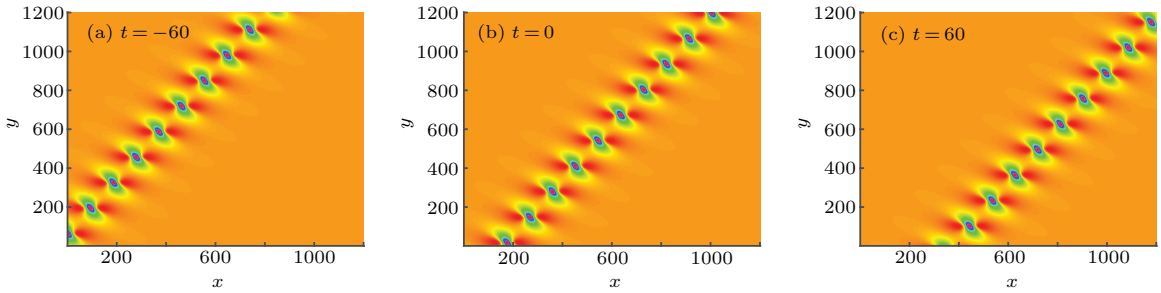


Fig. 9. The corresponding density plots for Fig. 8.

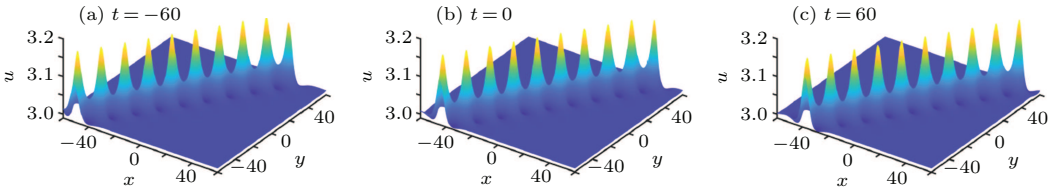


Fig. 10. Breather wave excited by the solution u_b with $\alpha=1$, $a_1=b_1=0.2$, $c_1=0.5$, $d_1=1.2$, $u_0=3$.

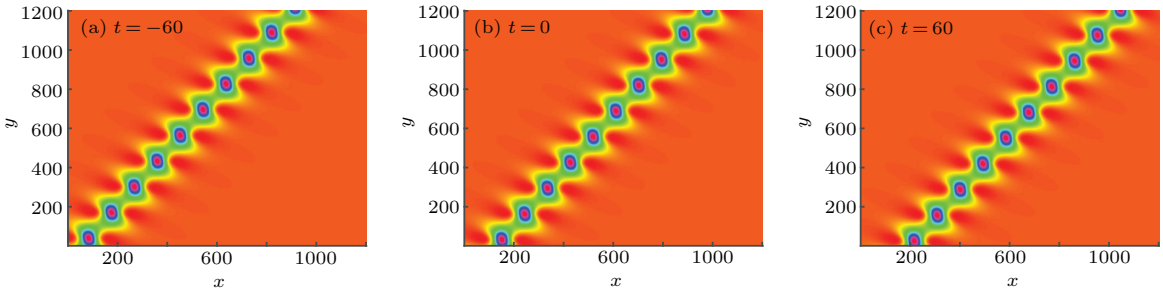


Fig. 11. The corresponding density plots for Fig. 10.

6. Conclusion

In this paper, with the help of the symbolic computation, the localized wave solutions of the (2+1)-dimensional HSI equation have been obtained. Among them, the rogue wave yielded by a lump soliton and a pair of resonance stripe solitons, and the fusion and fission phenomena generated by the lump solitons and one-stripe soliton. For the lump-type solution, it has been determined that the seed solution u_0 influences both the extreme value and the trajectory of the lump solutions. However, it only affects the speed of the breather wave but has no impact on their period.

Acknowledgement

Project supported by the National Natural Science Foundation of China (Grant Nos. 12275172 and 11905124).

References

[1] Chorin A J 1968 *Math. Comput.* **22** 745
[2] Constantin P and Foias C 1988 *Navier-Stokes Equations*, 2nd edn. (Chicago: Chicago University Press)
[3] Galdi G 2011 *An Introduction to the Mathematical Theory of the Navier-Stokes Equations: Steady-State Problems* (Luxembourg: Springer)
[4] Grue J, Jensen A, Rusås P O and Sveen J K 1999 *J. Fluid Mech.* **380** 257
[5] Koop C G and Butler G 1981 *J. Fluid Mech.* **112** 225
[6] Michallet H and Barthelemy E 1998 *J. Fluid Mech.* **366** 159
[7] Zabusky N J and Kruskal M D 1965 *Phys. Rev. Lett.* **15** 240
[8] Osman M S, Liu J G, Hosseini K, Lnc M and Yusuf A 2020 *Phys. Scr.* **95** 035229
[9] Zhang W X and Liu Y Q 2021 *AIMS Math.* **6** 11046
[10] Zahran E H M and Bekir A 2022 *Chin. J. Phys.* **77** 1236
[11] Zhang W X and Liu Y Q 2022 *Nonlinear Dyn.* **108** 2531
[12] Guo L J, Chen L, Mihalache D and He J S 2022 *Phys. Rev. E* **105** 014218
[13] Akinyemi L, Senol M, Tasbozan O and Kurt A 2022 *J. Ocean Eng. Sci.* **7** 536
[14] Zeng S J, Liu Y Q, Chen X and Zhang W X 2022 *Results Phys.* **42** 105992

[15] Chen M and Wang Z 2023 *Chin. Phys. B* **32** 090504
[16] Ablowitz M J and Satsuma J 1978 *J. Math. Phys.* **19** 2180
[17] Umeki M 1997 *Phys. Lett. A* **236** 69
[18] Yuan F, He J S and Cheng Y 2020 *Commun. Nonlinear Sci. Numer. Simul.* **83** 105027
[19] Zhao Z L and He L C 2021 *Appl. Math. Lett.* **111** 106612
[20] Vladimir I Kruglov and Houria Triki 2023 *Chin. Phys. Lett.* **40** 090503
[21] Ma W X 2015 *Phys. Lett. A* **379** 1975
[22] Wang H, Tian S F, Zhang T T and Chen Y 2019 *Front. Math. China* **14** 631
[23] Ismael H F, Murad M A S and Bulut H 2022 *Chin. J. Phys.* **77** 1357
[24] Zhang Z, Yang X, Li B, Guo Q and Stepanyants Y 2023 *Nonlinear Dyn.* **111** 1625
[25] Ma H C, Mao X and Deng A P 2023 *Chin. Phys. B* **32** 060201
[26] Zhang X E and Chen Y 2017 *Nonlinear Dyn.* **90** 755
[27] Liu J G and Zhao H 2022 *Chin. J. Phys.* **77** 985
[28] Chen J C and Zhu S D 2017 *Appl. Math. Lett.* **73** 136
[29] Chen J C, Ma Z Y and Hu Y H 2018 *J. Math. Anal. Appl.* **460** 987
[30] Kundu A, Mukherjee A and Naskar T 2014 *Proc. R. Soc. A* **470** 20130576
[31] Deng G F, Gao Y T, Ding C C and Su J J 2020 *Chaos, Solitons and Fractals* **140** 110085
[32] Hirota R 2004 *The Direct Method in Soliton Theory* (Cambridge: Cambridge University Press)
[33] Matveev V B and Salle M A 1991 *Darboux Transformation and Solitons* (Berlin: Springer-Verlag)
[34] Ablowitz M J, Kaup D J, Newell A C and Segur H 1974 *Stud. Appl. Math.* **53** 249
[35] Miura R M 1974 *Bäcklund Transformations, the Inverse Scattering Method, Solitons, and Their Applications* (Berlin: Springer)
[36] Hirota R and Satsuma J 1981 *Phys. Lett. A* **85** 407
[37] Hietarinta J 2004 *Integrability of Nonlinear Systems* **638** 95
[38] Zhou Y, Manukure S and Ma W X 2019 *Commun. Nonlinear Sci. Numer. Simul.* **68** 56
[39] Yan X Y, Liu J Z and Xin X P 2023 *Chin. Phys. B* **32** 070201
[40] Ma W X 2011 *Stud. Nonlinear Sci.* **2** 140
[41] Zhang X E and Chen Y 2017 *Commun. Nonlinear Sci. Numer. Simul.* **52** 24
[42] Wang S, Tang X and Lou S Y 2004 *Chaos, Solitons and Fractals* **21** 231
[43] Or-Roshid H and Rashidi M M 2017 *J. Ocean Eng. Sci.* **2** 120